Available online at www.sciencedirect.com
SCIENCE DIRECT
C. R. Geoscience 338 (2006) 161–171
COMPTES RENDUS GEOSCIENCE
http://france.elsevier.com/direct/CRAS2A/

Geomaterials (Sedimentology)

A survey of pyritised animal, plant, and trace fossils and concretionary pyrites, Germav Formation, southeastern Turkey

Cemal Bölücek *, Burhan Ilhan

Department of Geological Engineering, Engineering Faculty, Firat University, Elaziğ 23119, Turkey

Received 3 May 2005; accepted after revision 4 October 2005

Available online 18 January 2006

Presented by Ždenek Johan

Abstract

The sulphide-bearing rocks of the Upper Cretaceous Germav Formation in southeastern Turkey (Bozova–Urfa) and the morphologically varied sulphide occurrences they contain have been investigated. Pyrite and marcasite are the main sulphide minerals; lesser bravoite and millerite also occur. Pyritised branches and leaves, trace fossils, and animal microfossils and macrofossils are abundant. Most of the concretionary and authigenic concretionary pyrite occurrences are probably related to burrows. The concretionary pyrites have low Co and high Ni contents and low Co:Ni ratios. The pyrite-rich lithostratigraphic sequences were deposited in a deep-sea environment, and pyrite mineralization developed in syn-sedimentary, early diagenetic and epigenetic stages under anoxic conditions. ***To cite this article: C. Bölücek, B. Ilhan, C. R. Geoscience 338 (2006).***

Résumé

Une vue d'ensemble des animaux pyritisés, plantes, traces fossiles et pyrites concrétionnées de la formation de Germav (Sud-Est de la Turquie). Les roches à sulfures de la formation de Germav (Bozova–Urfa), dans le Sud-Est de la Turquie, d'âge Crétacé supérieur, ont été étudiées, ainsi que les gisements de sulfures, morphologiquement très variés, qu'elles contiennent. Pyrite et marcasite sont les espèces minérales les plus abondantes, à côté d'une quantité moins importante de bravoïte et de millérite. La plus grande partie des pyrites concrétionnées et/ou authigènes se trouvent à l'emplacement de terriers d'anciens animaux fouisseurs. Les pyrites concrétionnées ne contiennent que peu de Co, mais beaucoup de Ni, avec, par conséquent, de faibles rapports Co:Ni. Les séquences lithostratigraphiques riches en pyrite se sont déposées dans un environnement de mer profonde, et la minéralisation pyriteuse s'est développée lors d'épisodes syn-sédimentaires, diagénétiques précoces et épigénétiques, dans des conditions anoxiques. ***Pour citer cet article : C. Bölücek, B. Ilhan, C. R. Geoscience 338 (2006).***

Keywords: Concretionary pyrite; Co:Ni ratio; Southeastern Turkey; Trace fossil

Mots-clés : Pyrite concrétionnée ; Rapport Co:Ni ; Turquie du Sud-Est ; Traces fossiles

1. Introduction

Carbonate, sulphide, sulphate, phosphate and silica concretions, which occur in a variety of geological environments (e.g., lacustrine and marine sedimentary

* Corresponding author.
E-mail address: cbolucek@firat.edu.tr (C. Bölücek).

1631-0713/$ – see front matter
doi:10.1016/j.crte.2005.10.005

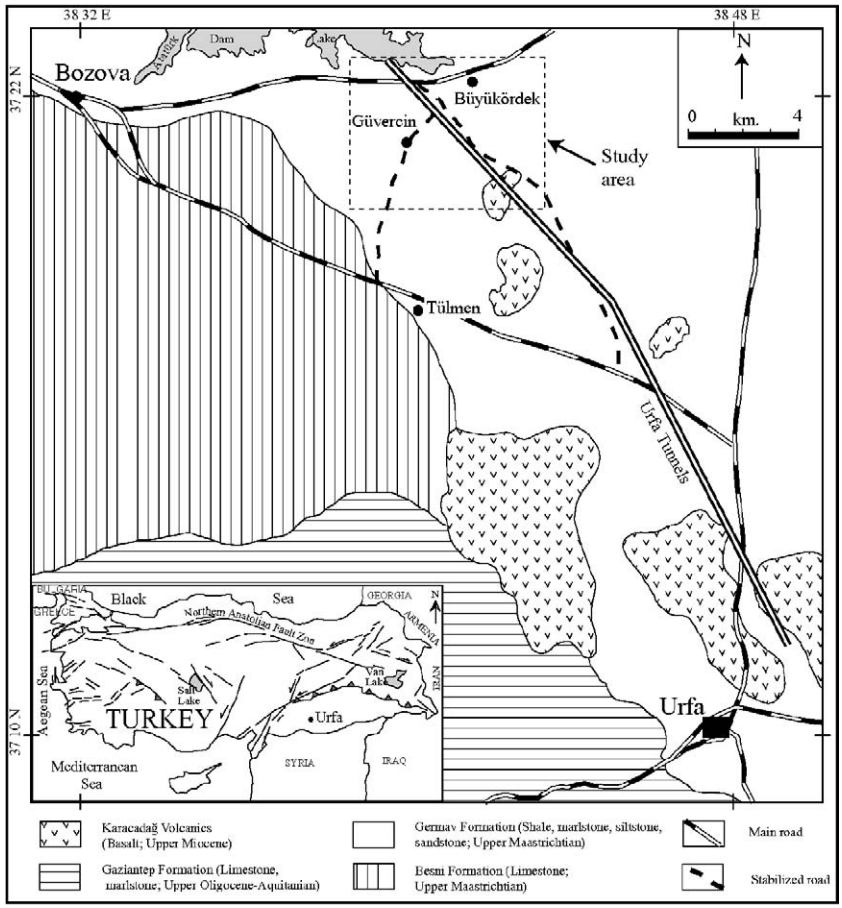

Fig. 1. General geological map of the district.

Fig. 1. Carte géologique général de la zone étudiée.

rocks), have been studied in a number of research programmes over the several last years [55]. Concretions record a short moment in the chemical progress of pore water, which becomes saturated with respect to the minerals that make up the concretion. They are said to be products of an early-diagenetic process. Sulphide concretions have been studied less than the others, especially from a morphological standpoint.

Our research has focussed initially on sulphide occurrences in the Germav Formation, in southeastern Turkey (Fig. 1). The sulphides therein predominantly comprise pyrite and marcasite. Pyritised plant and animal fossils, and interestingly shaped pyrite concretions (likely related to bioturbation structures) have been observed in the study area. In this article, the morphologies and mineralogical features of the pyrite concretions and their major- and trace-element contents have been considered. The overall major aspects of the pyrite concretions and pyritised plant, fish and trace fossils have been studied collectively in this research, thus differing from most other work on pyrite.

Pyrite is a mineral widespread in almost all geological environments. However, studies that have been carried out on pyrite occurrences in sedimentary environments have typically not emphasised morphology [1,4,5,11,12,16,26,27,32,36,37,41,60–65]. The most widely accepted view is that euhedral and framboidal pyrite forms in sedimentary environments under anoxic conditions.

2. Geological setting

The sulphide-bearing units considered in this study belong to the Upper Cretaceous Germav Formation (Fig. 1) [24]. The Germav Formation of southeastern Turkey is of varying thickness (35 to 1325 m) and is exposed over rather large areas [15]. The Germav Formation generally comprises siltstone and sandstone alter-

Fig. 2. Marlstone and bioturbated claystone succession.
Fig. 2. Succession de marnes et argilites à bioturbidites.

nating with greenish–grey shale and marlstone [66] and, locally, with conglomerate and detrital limestone [24]. Güven et al. [25] concluded that the Germav Formation formed in slope areas and submarine fans. Our own work in the same area corroborates that interpretation.

The Germav Formation comprises marlstone that contains the main pyrite concretions and bioturbated claystone that contains pyritised plant material (Fig. 2). At some levels, the unit is represented by chert-nodular limestone overlain by very thin sandstone layers. The sequence of claystone and marlstone layers reaches an apparent thickness of 150 m. Individual depositional layers have thicknesses between 50 and 100 cm. Sulphide-rich horizons, approximately 10-cm thick, occur locally within the sequence, and plant accumulations are also present in these sulphide-rich intervals.

The following fossils have been identified in the course of studies of samples taken from the Germav Formation. *Globotruncana linneiana* (d'Orbigny), *Globotruncana arca* (Cushman), *Globotruncanita stuarti* (de Lapparent), *Globotruncanita* cf. *stuartiformis* (Dalbiez), *Globotruncana* cf. *falsostuarti* (Dalbiez), *Globotruncana* cf. *Aegyptiaca* (Nakkady), *Globotruncanita* sp., *Globotruncanella* sp., *Rosita fornikata* (Plummer), *Rosita* sp., *Gansserina gansseri* (Bolli), *Heterohelix globulosa* (Ehrenberg), *Heterohelix* sp., Heterohelicidae, *Abathomphalus mayaroensis* (Bolli), *Abathomphalus* sp., *Pseudotextularia elegans* (Rzehak), *Praeglobotruncana* sp., *Rugoglobigerina* sp., *Globigerinelloides* sp. This fossil content indicates that the Germav Formation is of Late Maastrichtian age.

3. Materials and methods

The concretions related to pyritised plant remains, animal fossils and bioturbation structures examined in the present work were observed at different levels of the marl–claystone sequence. These occurrences are mostly oxidized as a result of surface alteration in the places from which samples were taken. In the study area, a tunnel has been dug for irrigation purposes at a depth of approximately 150 m below the marl–claystone sequence. It is possible to reach that tunnel via subtunnels from different points. Our samples were taken during excavation of the subtunnels. Therefore, the samples taken were fresh rock and sulphide samples that had not been subjected to any surface alteration.

The sulphide and various host-rock samples were studied microscopically. Thirty samples with concretionary characteristics, with varying proportions of pyrite and cement, were chemically analysed by ACME Laboratories, Canada. Inductively coupled plasma mass spectrometry (ICP-MS), inductively coupled plasma optic emission spectrometry (ICP-OES) and neutron activation analysis (NAA) were used to analyse the trace-element contents of the concretionary pyrite samples.

4. Sulphide occurrences and the morphological classification of pyrite

Various types of sulphide occurrences are abundant in the lithostratigraphic succession of marlstone, claystone and sandstone in the Germav Formation. These were studied in four groups: layered and lensoidal pyrites; pyritised plant and animal fossils; concretionary and authigenic pyrites.

4.1. Layered and lensoidal pyrites

Layered pyrites reach thicknesses of 10 cm, but there are also laminar intervals only a few millimetres in thickness near the marl–claystone contact. These occurrences are mainly fine-granular and massive, but there is also lesser disseminated pyrite. The lensoidal pyrites were also deposited as concordant layers, a few millimetres in thickness, in the sandy marls. Pyrites tend to either partially or completely enclose sandstone granules. In one place, another pyrite zone developed around pyrite that previously developed around a granule. There are also rounded pyrite granules. In most cases, the structure wraps around the sandstone granules, and the fossils are considered to be microconcretions that did not develop fully. Such pyrite occurrences are considered to have formed in either the sedimentary or early-diagenetic stages.

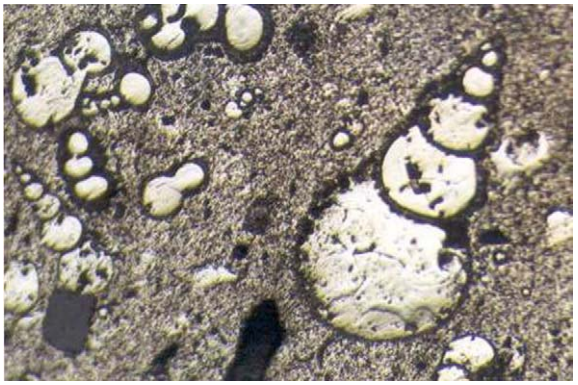

Fig. 3. Completely pyritised *Globutruncana* fossils in rings formed by cements of concretionary pyrites.

Fig. 3. Fossiles complètement pyritisés de *Globutruncana*, en anneaux formés par des ciments de pyrite concrétionnée.

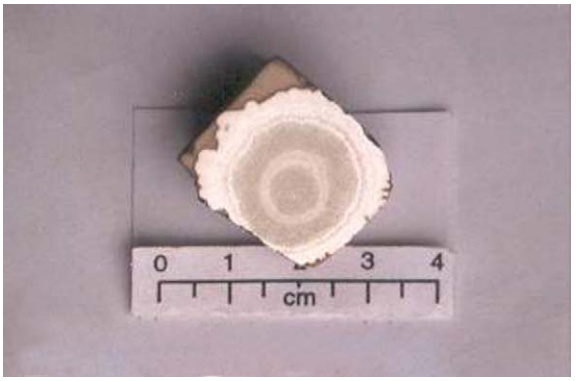

Fig. 4. Pyritic concretions showing ring-shaped, 'zigzag' occurrence due to octahedral crystal growth in the external part of a concretion.

Fig. 4. Concrétions pyriteuses annulaires, montrant un contour en « zigzag » en raison d'une croissance de cristaux octaédriques dans la partie externe de la concrétion.

4.2. Pyritised plant and animal fossils

While pyritised plants are found only in the claystone layers, pyritised animal fossils are concentrated in the marls. Pyritised animal fossils are more abundant in particular marl horizons. Of particular note are partially pyritised and rather well-preserved fish fossils, and non-pyritised macrofossils such as gastropods and bivalves. An abundance of pyritised plant branches and leaves are present in claystones at the base of the sequence. These plant-fossil accumulations comprise branches, 1–2 mm in diameter and 10–15 cm in length, or tree (trunk) pieces, 5 mm in diameter and 10 cm in length, with almost completely preserved bark and probable leaf pieces. The pyrites in the branches and leaves comprise rather fine granules. Some gastropod fossils are completely pyritised; however, the species have not been determined exactly. Moreover, some completely pyritised *Globotruncana* fossils occur in rings of cement in the concretionary pyrites (Fig. 3).

4.3. Concretionary pyrites

In the study area, the most widespread sulphide occurrences are concretions. The pyrite concretions are most abundant within shale that contains abundant organic material, and concretions also occur in marl intervals of the sequence that belongs to the Germav Formation. Such concretions developed in bioturbation structures and on transported tree fragments, and have tubular, spherical-ellipsoidal and cylindrical morphologies. The pyrite concretions formed when sulphide-bearing solutions filled cavities left by marine invertebrates that moved at or near the sediment–water interface during or just after sedimentation. Heterogeneity of the sediments may have played a role in the formation of the concretionary pyrites, as has been proposed for other concretions [8,9].

In the study area, tubular concretions are most abundant. These features are mostly perpendicular to but locally parallel layering; locally they are connected, but most are isolated from one another. The widths of the burrows vary from a few millimetres to 5 cm, and the lengths reach perhaps 3–4 cm and typically have an annular appearance. The rings are made up of massive pyrite and varying proportions of minerals and cements derived from the marls in which they are found. The inner parts of these concretions comprise repeating rings of fine granular and radial pyrite–marcasite crystals. Larger radial crystals occur in the outer parts of most specimens. The external surfaces of some specimens have been observed. These features were produced as a result of pyrite-filling of cavities produced by movement of organisms towards the sediment–water interface near the end of sedimentation and immediately prior to compaction. The external parts of some concretions have extended into the surrounding rock, and beautiful octahedral crystals have formed in these areas. Thus, the external parts of the concretions have a zigzag appearance (Fig. 4). These features form due to pressure of the developing crystal(s) onto proximal material at the outset of compaction. According to Seilacher [54], the pressure effect on the environs was probably obtained by means of pressurizing liquid cell or film of overpressured fluid in the development of the crystals.

Another commonly observed concretion type is the spherical-ellipsoidal. Such concretions occur in marls with normal bioturbation and average carbonate con-

Fig. 5. Pyrite concretions developed around transported tree fragments.

Fig. 5. Concrétions de pyrite développées autour de fragments transportés d'arbres.

Fig. 6. Concretions having a tree bark-like appearance.

Fig. 6. Concrétions dont l'aspect rappelle une écorce d'arbre.

Fig. 7. Late diagenetic or epigenetic euhedral pyrite.

Fig. 7. Pyrite euédrique de diagenèse tardive ou d'épigenèse.

tents. Locally, in some horizons, these types of concretions occur with chain-like forms, but most are independent of one another. In some cases, they are partially or completely rounded, but most are ellipsoidal. These concretions develop in cavities produced during vertical movement of organisms. The actual upward movement of organisms is apparently recorded locally. Spherical-ellipsoidal concretions comprise concentric rings 1 to 6 cm in diameter; such rings are largely persistent, but locally thin, and disappear. Each ring, more or less, presents an isotropic structure. Massive, fine-granular and radial pyrites occur, and rings made up of rock cements/matrices containing pyritised macroorganisms and microorganisms repeat once or more. On the other hand, there are concretions of this type made up only of pyrite and marcasite. These rings are single radial rings up to 1 cm in diameter, or multiple radial and random pyrite rings, 4 cm in diameter. Such concretions are generally accepted to have formed in the early-diagenetic stage [54]. When the mud is soft and still isotropic, a spherical lump around the burrow structure develops due to the addition of a layer, probably from the outside.

Abundant in the study area are cylindrical pyrite concretions that developed around transported tree fragments. Such concretions are 0.5 mm–1 cm in diameter and are an average of 4–5 cm in length (Fig. 5). The external surfaces of such concretions, up to 10 cm in length, have a tree bark-like appearance (Fig. 6). These concretions are made up only of pyrite and marcasite, and are characterised by an annular inner structure. Relatively well-preserved tree aspects indicate that such concretions may have formed in the early-diagenetic stage.

4.4. Authigenic pyrites

These pyrites are fracture-filling euhedral pyrites that probably formed both in the early- and late-diagenetic stages. While the euhedral pyrites of the early-diagenetic stage are abundant in the claystone intervals of the sequence, the late-diagenetic euhedral pyrites are mostly observed within the marl.

The early-diagenetic euhedral pyrites comprise cubic pyrite crystals varying from 10 μm to 1 cm in length, and typically occur as crystal accumulations, grown one over the other. Locally, concretions made up of rather fine radial pyrites become larger cubic pyrite crystals, reaching almost 1 cm in diameter, due to continuing growth. Such a situation reflects development of the local euhedral pyrite crystals, syngenetic with the concretions.

Late-diagenetic euhedral pyrites have cubic and octahedral forms. The fractures they fill resemble rosary beads arranged on a string (Fig. 7). These euhedral pyrites comprise diagenetic pyrites – redissolved and re-

crystallised in cracks and fractures after the compaction of the rocks – and thus are clearly post-sedimentation features.

5. Mineralogical investigation of the sulphide mineral occurrences

During the course of reflected light microscopy of the concretionary and other sulphide occurrences, pyrite and marcasite were recognised as the dominant minerals. Bravoite, millerite and their alteration product, violarite, were identified in the central parts of some concretions.

Pyrite (FeS_2): The most abundant sulphide mineral in the study area, pyrite is mainly observed in concretionary form, but also occurs as cubic and octahedral crystals, varying in size from a few microns to a few millimetres (coarse granules). The concretionary pyrites mainly possess radial textures.

Marcasite (FeS_2): The second most abundant sulphide mineral in the study area is marcasite, and it typically occurs with interpenetrating texture. Strong colour anisotropy of the marcasites (green, brown, grey) facilitates their recognition. Some of the marcasites are partially or completely altered to violarite.

Marcasite is a form of FeS_2 that forms at low temperature and under acidic conditions [13]. Marcasite crystallises more readily than pyrite at low pH (less than 5) and at low temperatures (under 75 °C) [40]. Various researchers report that marcasite forms via conversion of the leading ferrous sulphur, and that marcasite is not directly precipitated from the solution. Benning et al. [3] pointed out that in the formation of the marcasite, polysulphide concentration (more than 10^{-5} to 10^{-6} molar) is important, as are pH and temperature. Marcasite generally forms as a replacement of concretions or fossils in adequately reducing environments; however, it may also form by conversion of pyrite at the onset of very acidic conditions. In such cases, pyrite and marcasite may be intergrown [58].

Bravoite (Fe, Ni, CoS_2): Lesser amounts of bravoite are encountered in some samples. Generally, pyrite and locally marcasite seem to have a zoned structure. Pyrite may accommodate Ni and Co in the Fe position of the crystal structure. Increase in Ni allows crystallisation of bravoite, and unit cell size also increases in response to increasing Ni content [58].

Millerite (NiS): Another sulphide mineral present in minor amounts is millerite, which mainly occurs as elongate rods. Locally violarite (Ni_2FeS_4) is an alteration product at grains margins and as plates. It is thought that millerite formed by alteration of nickeliferous pyrites instead of by direct precipitation from pore waters.

6. Chemical composition of the pyrite concretions

Various trace elements may be concentrated in pyrites of different origin [16]. The concentration of metals in pyrite depends on the concentrations of the various metals in the precipitation environment. Metals that may circulate in a hydrologic column become fixed in sediments rich in organic material [51].

Many elements, such as Cu, Zn, As, Sb, Ni and Co, may be highly concentrated in sedimentary rocks, especially in anoxic sediments [63]. For example, jointly precipitated As and Co may be concentrated in Fe-sulphides in such environments [33,57]. The enrichment of Cd in anoxic sediments is clearly related to the sulphide fraction [31,56]. Furthermore, Zn is related to the sulphides in sediments [19], and significant Ni also occurs in sedimentary pyrites [35,44]. Stoichiometrically, Ni and Co in pyrite replace ferrous iron, and Se and Te replace sulphur [30]. In fact, these elements tend to be concentrated in pyrite and marcasite, the main sulphide phases in such environments [51].

Trace elements in pyrite, such as Ag, Pb, Cu, Mn, Ti and Ni, may aid in elucidation of ore genesis [49]. However, the Co and Ni contents of pyrites or, more specifically, their Co:Ni ratios, are primarily used as indicators of ore genesis [7,22,23,34,50,62]. Hydrothermal pyrites have extremely variable Co and Ni contents and rather variable Co:Ni ratios. Pyrites in massive sulphide deposits have Co:Ni ratios of 5–50 (average 8.7), with high Co contents (average 480 ppm) and Ni contents less than 100 ppm (average 56 ppm) [7]. Sedimentary pyrites in shale have high Ni contents [34] and low Co:Ni ratios (average 0.63) [7].

Our analytical results from the concretions (Tables 1 and 2) indicate that mineralogical components other than sulphide phases (pyrite ∼80%) are also present in significant amounts (∼20%). Major oxides, such as Al, Ca, K, Mg, Na and Si (not analysed, probably) may have been derived from the host-rock cement that binds the concretions. Apart from the sulphide cements, the clay-fraction minerals comprise carbonates and probably quartz grains. In addition to those major oxides, trace elements of lithophilic character, such as Zr and Sn, may have been concentrated in other (non-sulphide) components within the concretions. Of course, elements such as Ni, Co, Zn and Cu tend to be enriched in sulphide minerals [19,28,29].

It is well known that Co and Ni are enriched in pyrite and marcasite in the sedimentary environment.

Table 1
Major-element contents (in wt%) of pyrite concretions

Tableau 1
Teneur en éléments majeurs (en poids %) des concrétions pyriteuses

Samples	Al	Ca	K	Mg	Na	P	Ti	Fe	S
B-1	0.3	0.31	0.10	0.04	0.042	0.002	0.024	44.0	42.5
B-2	0.4	0.25	0.13	0.05	0.026	0.003	0.032	41.6	38.9
B-3	0.32	0.07	0.09	0.03	0.028	0.001	0.027	39.8	36.4
B-4	0.26	0.44	0.08	0.03	0.038	0.005	0.022	39.7	36.8
B-5	0.30	0.34	0.09	0.04	0.024	0.005	0.029	39.0	35.8
B-6	0.36	0.55	0.11	0.04	0.037	0.009	0.030	38.6	37.1
B-7	0.18	0.12	0.05	0.02	0.022	0.006	0.015	40.2	37.7
B-8	0.26	0.30	0.09	0.03	0.030	0.008	0.023	38.8	36.6
B-9	0.23	0.29	0.07	0.03	0.026	0.007	0.020	40.3	38.0
B-10	0.27	0.26	0.09	0.04	0.030	0.002	0.026	39.8	37.1
B-11	0.26	0.11	0.08	0.03	0.028	0.004	0.024	40.0	37.2
B-12	0.21	0.39	0.07	0.03	0.031	0.008	0.021	41.1	39.0
B-13	0.16	0.17	0.05	0.02	0.017	0.006	0.016	43.0	39.6
B-14	0.22	0.41	0.07	0.03	0.044	0.002	0.021	40.1	36.6
B-15	0.09	3.88	0.04	0.06	0.023	0.005	0.009	36.1	37.6
B-16	0.21	0.24	0.06	0.03	0.031	0.005	0.021	38.2	43.5
B-17	0.30	0.27	0.09	0.04	0.023	0.003	0.029	40.6	40.7
B-18	0.22	0.23	0.07	0.03	0.030	0.002	0.023	39.3	38.6
B-19	0.21	0.47	0.07	0.03	0.024	0.002	0.023	39.4	39.2
B-20	0.33	0.20	0.11	0.04	0.050	0.002	0.031	39.5	38.8
B-21	0.20	0.25	0.07	0.03	0.019	0.001	0.021	41.2	40.5
B-22	0.14	0.09	0.04	0.02	0.033	<0.001	0.015	42.4	40.1
B-23	0.23	0.24	0.07	0.03	0.030	0.001	0.024	40.5	40.2
B-24	0.20	0.26	0.06	0.03	0.024	<0.001	0.022	41.8	40.9
B-25	0.10	0.08	0.03	0.01	0.019	<0.001	0.013	41.7	46.6
B-26	0.24	0.35	0.07	0.03	0.035	<0.001	0.024	39.8	41.7
B-27	0.15	0.27	0.05	0.02	0.025	<0.001	0.017	40.3	40.4
B-28	0.17	0.19	0.06	0.03	0.043	0.002	0.016	40.1	41.6
B-29	0.25	0.20	0.09	0.03	0.032	<0.001	0.025	39.3	40.5
B-30	0.32	3.49	0.22	0.06	0.039	<0.001	0.037	38.0	40.3

In the studied concretions, pyrite, bravoite (the nickeliferous form of pyrite) and marcasite are the main sulphide phases. Millerite and violarite occur in trace amounts in only a few samples. In sedimentary pyrites, there is typically a strong correlation between Co and Ni ($r = 0.93$; [7]), but their correlation is weaker in the study area ($r = 0.77$), probably due to the fact that they were derived from local materials; alternatively, these metals may have been redistributed. Co values of the concretions are rather low (range 3–12; average 12), but Ni contents are rather high (range 29–253.7; average 91.54). The Co:Ni values (average = 0.06) of the concretionary pyrites from the study area are rather low compared to pyrites of other environments (Fig. 8). These data indicate that the studied pyrites are of sedimentary origin.

7. Discussion and conclusions

Pyrite assumes mainly framboidal or euhedral forms in sedimentary environments. Framboids form under acidic conditions [38] through precipitation [60] of micron-sized pyrite crystals. On the other hand, the euhedral pyrite comprises micron-sized crystals [41,42] that develop under neutral-alkali conditions [38]. Framboidal pyrites develop indirectly from ferrous monosulphides (amorphous FeS, mackinawite, greigite, pyrite) [53,60,64]. Such conversions occur through rather rapid processes [46]. Conversion from greigite into pyrite can occur either via addition of sulphur [4] or by loss of ferrous iron [20]; euhedral pyrites are formed from pore water saturated with respect to ferrous monosulphides [39,48]. Indirect crystallisation occurs via high activity of (dissolved) sulphides, and with the kinetic activity of ferrous monosulphides; framboidal pyrite develops in the early-diagenetic stage [17]. On the other hand, euhedral pyrite precipitates directly [21,45,53]. The euhedral pyrites are saturated with respect to pyrite, but are precipitated from pore water, which is not saturated with respect to monosulphides [47,63]. Euhedral pyrites form from pore water having depleted sulphide ratios in a late stage of early diagenesis [14], but form during early diagenesis when the sulphate reduction rate is low [61].

Framboidal pyrites have not been observed in the study area. However, it is thought that concretionary pyrite occurrences in the study area may have initially precipitated as framboids. Sawlowicz [51] points out that there are many similarities between concretions and framboids. According to that worker, probably in the early stages of concretion formation, the components (crystals) that make up the concretions have framboidal textures (polyframboids), or at least framboidal nuclei. The dimensions of framboids increase via the formation of pyrite euhedra.

A close relationship between pyrite formation and organic material was observed in the study area, as demonstrated by the presence of biogenic materials, such as animal macrofossils and microfossils, and fossilised tree branches and leaves, in bioturbated claystones and marls of the area. Indeed, organic materials in natural sedimentary environments are critical to pyrite crystallisation. The main source of sulphur for development of ferrous sulphides in sedimentary environments is H_2S or HS^- derived from bacterial sulphate reduction (Fig. 9) [4,51]. Round–oval masses observed in concretions are evidence of local sulphate reduction [52]. The bacteria that reduce sulphate do not precipitate sulphides directly; their role is probably limited to production of bisulphide ions [2]. Pyritised fossils, widespread in the study area, may be interpreted as the replacement of organic material by pyrite [10]. The replacement of soft parts occurs in sediments near the

Table 2
Trace-element contents (Au in ppb; others in ppm) of pyrite concretions. Italicised bold numbers indicate elements analysed by NAA

Tableau 2
Teneur en éléments en trace contents (Au en ppb ; les autres in ppm) des concrétions pyriteuses. Les chiffres en italiques gras indiquent des éléments analysés par activation neutronique (NAA)

Samples	***Au***	Ag	***As***	***Co***	Cu	Mo	Ni	Pb	Zn	Ba	Cr	La	Mn	Nb	Rb	***Sc***	Sr	Th	V	Y	Zr
B-1	**6**	0.1	***<0.5***	8	14	0.3	154	5.4	18	9	14	0.8	65	0.6	4.1	***0.9***	17	0.2	1	0.7	3.7
B-2	**5**	0.1	***1.4***	7	10	0.3	145	5.3	27	8	17	1.3	126	0.9	5.5	***1.4***	18	0.3	3	1.2	4.3
B-3	**6**	0.2	***0.9***	4	8	0.3	29	2.5	30	7	14	0.8	170	0.9	4.1	***0.9***	9	0.2	6	0.8	3.1
B-4	**6**	0.1	***1.5***	6	10	2.3	107	13.6	39	11	16	0.8	168	0.8	3.1	***0.8***	19	0.2	2	0.7	3.1
B-5	**24**	0.2	***1.2***	6	10	0.2	94	4.6	35	9	14	1.1	244	0.9	4.1	***1***	20	0.2	<1	0.8	4.5
B-6	**29**	0.1	***1.4***	5	17	3.3	154	11	35	15	24	1.3	334	0.9	5.5	***1.4***	24	0.3	2	1.1	5.1
B-7	**<2**	<0.1	***<0.5***	4	5	0.1	36	2.5	18	6	8	0.6	62	0.4	2	***0.7***	9	0.1	2	0.5	1.7
B-8	**10**	0.1	***0.9***	5	12	2.3	63	10.1	28	8	17	0.9	152	0.8	3.8	***0.9***	16	0.2	<1	0.6	3.6
B-9	**7**	<0.1	***0.9***	6	6	0.2	98	2.7	27	9	12	0.7	131	0.7	3.4	***0.9***	15	0.2	2	0.9	2.8
B-10	**5**	0.1	***1.1***	5	12	2.5	112	11.8	29	21	18	0.7	163	0.6	4.1	***1***	16	0.2	<1	0.8	4.7
B-11	**9**	<0.1	***<0.5***	4	8	0.2	67	4.2	29	7	14	0.8	128	0.7	3.7	***1***	11	0.2	2	0.6	4
B-12	**8**	0.1	***<0.5***	7	10	3.8	96	5.9	30	9	18	0.7	147	0.6	2.9	***0.8***	17	0.1	1	0.5	2.7
B-13	**<2**	<0.1	***0.9***	4	6	0.1	71	3.3	18	7	9	0.6	46	0.5	2.8	***0.6***	10	0.1	<1	0.6	1.6
B-14	**10**	0.1	***<0.5***	6	11	3.1	110	7.6	28	8	19	0.8	172	0.6	3.1	***0.9***	17	0.2	<1	0.6	3.7
B-15	**6**	0.1	***<0.5***	3	4	0.2	68	6.1	15	11	6	0.7	59	0.3	1.5	***0.5***	86	0.1	1	0.8	1.6
B-16	**<2**	0.1	***1.2***	6	10	3	54	4.8	18	5	17	0.7	69	0.6	2.9	***0.7***	12	0.1	<1	0.5	3.5
B-17	**10**	<0.1	***<0.5***	5	10	0.1	85	3.2	26	7	15	0.8	137	0.8	4.5	***1.1***	17	0.3	2	0.9	3.9
B-18	**6**	0.1	***1.4***	6	11	3.7	68	5.6	20	8	20	0.7	92	0.6	2.9	***0.9***	13	0.1	2	0.7	2.3
B-19	**18**	0.2	***1.5***	5	9	0.1	65	4.2	32	9	11	0.8	290	0.9	3.3	***0.8***	20	0.1	1	0.8	2.9
B-20	**17**	0.1	***<0.5***	6	12	2.9	68	4.6	29	7	25	0.9	264	1.1	4.8	***1.4***	14	0.2	<1	1	6.9
B-21	**5**	<0.1	***<0.5***	5	7	0.2	111	2.7	13	9	12	0.7	34	0.6	3.1	***0.8***	12	0.2	3	0.8	3.7
B-22	**<2**	0.1	***<0.5***	5	17	3.5	107	6.5	17	6	14	0.4	70	0.4	2	***0.5***	6	0.1	3	0.4	2.9
B-23	**16**	0.1	***0.9***	4	7	0.1	80	3.2	31	8	13	0.8	201	0.9	3.2	***0.8***	14	0.2	<1	0.7	3.4
B-24	**<2**	0.1	***<0.5***	7	15	2.4	114	5.4	15	7	17	0.6	68	0.8	2.8	***0.6***	14	0.2	<1	0.7	2.9
B-25	**3**	0.1	***<0.5***	4	12	0.1	56	3.6	16	5	6	0.3	33	0.5	2.1	***0.4***	4	<0.1	2	0.2	2
B-26	**18**	0.1	***1***	5	10	3.5	81	3.6	28	8	22	0.7	153	0.7	4.6	***0.8***	16	0.2	1	0.6	3
B-27	**11**	0.1	***<0.5***	4	6	0.1	34	2.7	30	9	9	0.4	194	0.6	3	***0.6***	12	0.1	<1	0.5	2.6
B-28	**4**	<0.1	***<0.5***	4	8	2.4	56	4	23	9	14	0.6	96	0.4	2.3	***0.7***	11	0.1	1	0.6	2.7
B-29	**<2**	<0.1	***<0.5***	3	4	0.2	112	3.1	35	8	13	0.7	323	0.8	4.2	***0.9***	13	0.2	<1	0.7	3.4
B-30	**33**	1.2	***1.4***	12	159	1.3	254	18.2	23	20	43	1.7	140	1.2	5.3	***1.2***	91	0.3	<1	1.4	8

sediment–water interface during diagenesis, in which bacterial sulphate reduction is relatively slow and ferrous iron is dominant [13,43]. Moreover, few anaerobic environments are the most suitable for pyritisation of fossils [18].

The types of trace fossils that may have played important roles in the formation of pyrites in the study area could not be determined unequivocally. Ekdale and Bromley [17] pointed out that Upper Cretaceous marine-shelf chalks are rich in trace fossils; the most abundant were crustacean burrows (e.g., thalassonoids), but feeding/dwelling burrows of worms and other organisms (e.g., chondrites, zoophycos and planolites) were also quite widespread. Those researchers also reported that secondary mineralisation (replacement) of trace fossils is a typical characteristic of marine self chalks, and that pyritised trace fossils occur much more characteristically in marl–chalk facies (i.e., those rich in clay). However, Stow et al. [59] indicated that burrow types in deep water typically include zoophycos, planolites, and chondrites (ichnogenera). The sedimentary facies and trace-fossil contents of the Germav Formation suggest that it was deposited in a deep-sea environment.

The Co contents of the studied concretionary pyrites are rather low, but the Ni contents are high. The Co:Ni ratios of the pyrites are approximately 0.06. This value is rather characteristic of sedimentary pyrites. Furthermore, these data indicate that no magmatic or volcanic activity was operative in the formation of the pyrites. Moreover, there is no other evidence for magmatic or volcanic activity in this region.

In conclusion, we suggest that – on the basis of the sedimentological and stratigraphic features of the Germav Formation and the evaluation of the microscopic and geochemical data – the pyrite occurrences formed under anoxic conditions, through direct and indirect precipitation of seawater in association with organic material. The layered and lensoidal pyrites are syngenetic,

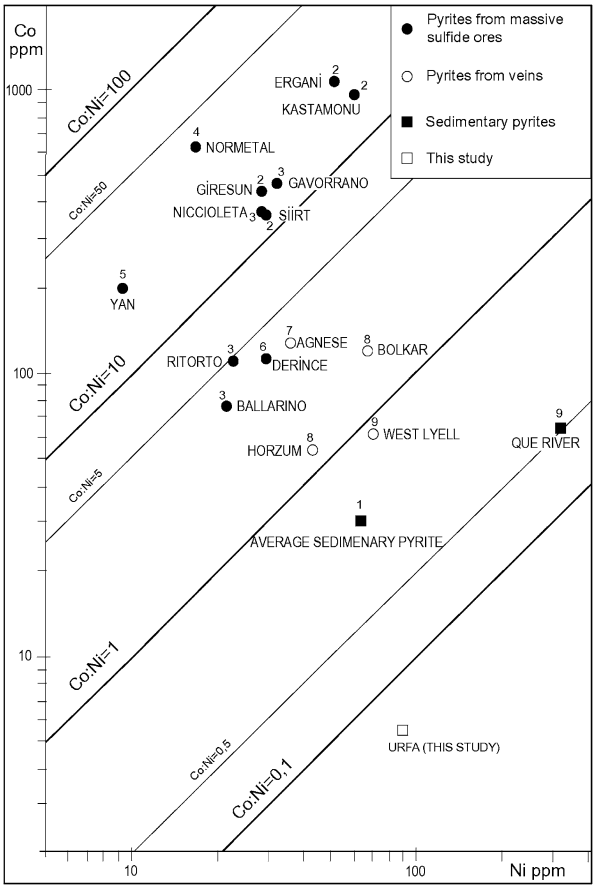

Fig. 8. Co versus Ni plots of average values of pyrites from various ores. (**1**) Average of sedimentary pyrites (after [7]); (**2**) pyrites from massive sulphide ores, Turkey, Kastamonu 7 samples, Ergani 6 samples, Giresun 12 samples, Siirt 8 samples [23]; (**3**) Tuscany massive sulphide ores, Italy, Gavorrano 8 samples, Niccioleta 9 samples, Ritorto 107 samples, Ballerino 89 samples [7]; (**4**) Normetal, Canada, 12 samples (after [7]); (**5**) Yanahara, Japan, 19 samples (after [7]); (**6**) Derince, Turkey, 30 samples [6]; (**7**) Agnese, Italy, 6 samples (after [7]); (**8**) vein-type ores, Turkey, Horzum 32 samples, Bolkar 56 samples [62]; (**9**) West Tasmania, Australia, West Lyell, 8 samples, Que River, 9 samples [34].

Fig. 8. Relations Co:Ni dans les teneurs moyennes des pyrites de minéralisations variées. (**1**) Moyenne des pyrites sédimentaires (d'après [7]) ; (**2**) pyrites d'amas sulfurés massifs, Turquie, Kastamonu 7 échantillons, Ergani 6 échantillons, Giresun 12 échantillons, Siirt 8 échantillons [23] ; (**3**) amas sulfurés massifs de Toscane, Italie, Gavorrano 8 échantillons, Niccioleta 9 échantillons, Ritorto 107 échantillons, Ballerino 89 échantillons [7] ; (**4**) Normetal, Canada, 12 échantillons (d'après [7]) ; (**5**) Yanahara, Japon, 19 échantillons (d'après [7]) ; (**6**) Derince, Turquie, 30 échantillons [6] ; (**7**) Agnese, Italie, 6 échantillons (d'après [7]) ; (**8**) minerais filoniens, Turquie, Horzum 32 échantillons, Bolkar 56 échantillons [62] ; (**9**) Tasmanie occidentale, Australie, West Lyell, 8 échantillons, rivière Que, 9 échantillons [34].

the concretionary and authigenic pyrites are early diagenetic, and the fracture-fill pyrites are of epigenetic origin.

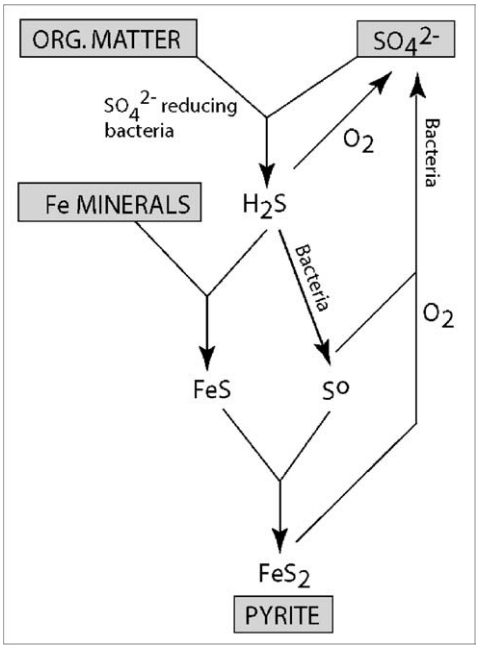

Fig. 9. Diagramatic representation of the process of pyrite formation (after [4]).

Fig. 9. Diagramme représentant le processus de formation de la pyrite (d'après [4]).

Acknowledgements

This study was funded by the Scientific Research Fund of Firat University (FÜBAP, Project No. 664). We are grateful to Prof. Dr. Izver Özkar (Istanbul University) for fossil determinations. We thank Dr. Steve Mittwede for critical reading and suggestions for improving early version of the manuscript.

References

[1] T.F. Anderson, J. Kruger, R. Raiswell, C–S–Fe relationships and the isotopic composition of pyrite in the New Albany Shale of the Illinois Basin, USA, Geochim. Cosmochim. Acta 51 (1987) 2795–2805.

[2] L.G. Benning, R.T. Wilkin, K.O. Konhauser, Iron monosulphide stability: experiments with sulphate-reducing bacteria, in: H. Armannsson (Ed.), Proc. Int. Symp. on the Geochemistry of Earth's Surface, vol. 5, 1999, pp. 429–432.

[3] L.G. Benning, R.T. Wilkin, H.L. Barnes, Reaction pathways in the Fe–S system below 100 °C, Chem. Geol. 167 (2000) 25–51.

[4] R.A. Berner, Sedimentary pyrite formation: an update, Geochim. Cosmochim. Acta 48 (1984) 605–615.

[5] C. Boesen, D. Postma, Pyrite formation in anoxic environments of the Baltic, Am. J. Sci. 288 (1988) 575–603.

[6] C. Bölücek, M. Akgül, S. Temur, The effect to the results of chemical analyses method: an example from Derince (Elazığ) pyrites, Geosound 39 (2001) 31–38.

[7] A. Bralia, G. Sabatini, F. Troja, A revaluation of the Co/Ni ratio in pyrite as geochemical tool in ore genesis problems, Mineral. Deposita 14 (1979) 353–374.

[8] J.-G. Bréhéret, Phosphatic concretions in black facies of the Aptian–Albian Marnes bleues Formation of the Vocontian basin (SE France), and at site DSDP 369: evidence of benthic microbial activity, Cretaceous Res. 12 (1997) 411–435.

[9] J.-G. Bréhéret, H.J. Brumsack, Barite concretions as evidence of pauses in sedimentation in the Marnes Bleues Formation of the Vocontian Basin (SE France), Sediment. Geol. 130 (2000) 205–228.

[10] D.E.G. Briggs, S.H. Bottrell, R. Raiswell, Pyritisation of soft-bodied fossils: Beecher's Trilobite bed, Upper Ordovician, New York State, Geology 19 (1991) 1221–1224.

[11] S.E. Calvert, H.G. Thode, D. Yeung, R.E. Karlin, A stable isotope study of pyrite formation in the Late Pleistocene and Holocene sediments of the Black Sea, Geochim. Cosmochim. Acta 60 (1996) 1261–1270.

[12] D.E. Canfield, Isotopic fractionation by natural populations of sulfate-reducing bacteria, Geochim. Cosmochim. Acta 65 (2001) 1117–1124.

[13] D.E. Canfield, R. Raiswell, Pyrite formation and fossil preservation, in: P.A. Allison, D.E.G. Briggs (Eds.), Taphonomy: Releasing the Data Locked in the Fossil Record, Top. Geobiol. 9 (1991) 337–387.

[14] M.I. Coleman, R. Raiswell, Source of carbonate and origin of zonation in pyritiferous carbonate concretions: evaluation of a dynamic model, Am. J. Sci. 295 (1995) 282–308.

[15] T. Çoruh, H. Yakar, N.Ş. Ediger, Güneydoğu Anadolu Bölgesi Otokton Istifinin Biyostratigrafi Atlasi, TPAO Araştırma Merkazi Grubu Baskanligi, No. 30, 1997, 401 p.

[16] J.R. Craig, F.M. Vokes, T.N. Solberg, Pyrite: physical and chemical textures, Mineral. Deposita 34 (1998) 82–102.

[17] A.A. Ekdale, R.G. Bromley, Comparative ichnology of shelf-sea and deep-sea chalk, J. Paleontol. 58 (1984) 322–332.

[18] I.St.J. Fısher, J.D. Hudson, Pyrite geochemistry and fossil preservation in shales, Phil. Trans. R. Soc., Lond. B 311 (1985) 167–169.

[19] M. Fleischer, Minor elements in some sulfide minerals, in: A.M. Bateman (Ed.), Econ. Geol. (50th Anniversary Volume, 1905–1955, part 2), 1955, pp. 970–1024.

[20] Y. Furukawa, H.L. Barnes, Reaction forming pyrite from precipitated amorphous ferrous sulfide, in: M.A. Vairavamurthy, M.A.A. Schoonen (Eds.), Geochemical Transformations of Sedimentary Sulfur, Am. Chem. Soc., 1995, pp. 194–205.

[21] M.B. Goldhaber, I.R. Kaplan, The sulfur cycle, in: E.D. Goldberg (Ed.), The Sea, vol. 5, Wiley, New York, 1974, pp. 569–655.

[22] G.J.S. Govett, T.M. Pantazis, Distribution of Cu, Zn, Ni and Co in the Troodos Pillow Lava Series, Cyprus, Trans. Inst. Min. Met. 80 (1971) B27–B46.

[23] N. Güleç, A. Erler, Masif sülfid yataklarındaki piritlerin karakteristik iz element içerikleri, Türkiye Jeol. Kur. Bült. 26 (1983) 145–152.

[24] Y. Günay, Güneydogu Anadolu'nun jeoljisi, stratigrafisi, TPAO Rapor, 1998, 227 p.

[25] A. Güven, A. Dinçer, M.E. Tuna, T. Çoruh, Güneydogu Anadolu Kampaniyen-Paleosen otokton istifin stratigrafisi, TPAO Arama Rapor No. 2828, 1991, 133 p.

[26] K.S. Habicht, D.E. Canfield, Sulfur isotope fractionation during bacterial sulfate reduction in organic-rich sediments, Geochim. Cosmochim. Acta 61 (1997) 5351–5361.

[27] K.S. Habicht, D.E. Canfield, Isotope fractionation by sulfate-reducing natural populations and the isotopic composition of sulfide in marine sediments, Geology 29 (2001) 555–558.

[28] M.A. Huerta-Diaz, J.W. Morse, A quantitative method for determination of trace metal concentrations in sedimentary pyrite, Mar. Chem. 29 (1990) 119–144.

[29] M.A. Huerta-Diaz, J.W. Morse, Pyritization of trace metals in anoxic marine sediments, Geochim. Cosmochim. Acta 56 (1992) 2681–2702.

[30] D.L. Huston, M. Power, J.B. Gemmell, R.R. Large, Design, calibration and geological application of the first operational Australian laser ablation sulphur isotope microprobe, Aust. J. Earth Sci. 42 (1995) 549–555.

[31] L. Jacobs, S. Emerson, J. Skei, Partitioning and transport of metals across the O_2/H_2S interface in a permanently anoxic basin: Framvaren Fjord, Norway, Geochim. Cosmochim. Acta 49 (1985) 1433–1444.

[32] M.J. Kohn, L.R. Riciputi, D. Stakes, D.L. Orange, Sulfur isotope variability in biogenic pyrite: reflections of heterogeneous bacterial colonization?, Am. Mineral. 83 (1998) 1454–1468.

[33] W.M. Landing, B.L. Lewis, in: E. Izdar, J.W. Murray (Eds.), NATO–ASI Symposium Series 'Black Sea Oceanography', 1991, pp. 125–160.

[34] G. Loftus-Hills, M. Solomon, Cobalt, nickel and selenium in sulphides as indicators of ore genesis, Miner. Deposita 2 (1967) 228–242.

[35] G.W. Luther III, T.M. Church, J.R. Scudlark, M. Cosman, Inorganic and organic sulfur cycling in salt-marsh pore-waters, Science 232 (1986) 746–748.

[36] T.W. Lyons, Sulfur isotopic trends and pathways of iron sulfide formation in Upper Holocene sediments of the anoxic Black Sea, Geochim. Cosmochim. Acta 61 (1997) 3367–3382.

[37] J.L. McKay, F.J. Longstaffe, Sulphur isotope geochemistry of pyrite from the Upper Cretaceous Marshybank Formation, Western Interior Basin, Sediment. Geol. 157 (2003) 175–195.

[38] J.W. Morse, Q. Wang, Pyrite formation under conditions approximating those in anoxic sediments. II. Influence of precursor iron minerals and organic matter, Mar. Chem. 57 (1997) 187–193.

[39] J.W. Morse, F.J. Millero, J. Cornwell, D.T. Rickard, The chemistry of the hydrogen sulfide and iron sulfide systems in natural waters, Earth-Sci. Rev. 24 (1987) 1–42.

[40] J. Murowchick, H. Barnes, Marcasite precipitation from hydrothermal solutions, Geochim. Cosmochim. Acta 50 (1986) 2615–2629.

[41] H.F. Passier, J.J. Middelburg, G.J. Lange, M.E. Böttcher, Pyrite contents, microtextures, and sulfur isotopes in relation to formation of the youngest eastern Mediterranean sapropel, Geology 25 (1997) 519–522.

[42] R. Raiswell, Pyrite texture, isotopic composition and the availability of iron, Am. J. Sci. 282 (1982) 1244–1263.

[43] R. Raiswell, A geochemical framework for the application of stable sulphur isotopes to fossil pyritization, J. Geol. Soc. Lond. 154 (1997) 343–356.

[44] R. Raiswell, J. Plant, The incorporation of trace elements into pyrite during diagenesis of Black Shales, Yorkshire, England, Econ. Geol. 75 (1980) 684–699.

[45] D.T. Rickard, Kinetics and mechanism of pyrite formation at low temperatures, Am. J. Sci. 275 (1975) 636–652.

[46] D.T. Rickard, Experimental concentration-time curves for the iron (II) sulphide precipitation process in aqueous solutions and their interpretation, Chem. Geol. 78 (1989) 315–324.

[47] D.T. Rickard, Kinetics of pyrite formation by the H_2S oxidation of iron (II) monosulphide in aqueous solutions between 25 and 125 °C: the rate equation, Geochim. Cosmochim. Acta 61 (1997) 115–134.

[48] A.P. Roberts, G.M. Turner, Diagenetic formation of ferrimagnetic iron sulphide minerals in rapidly deposited marine sediments, South Island, New Zealand, Earth Planet. Sci. Lett. 115 (1993) 257–273.

[49] F.I. Roberts, Trace element chemistry of pyrite: a useful guide to the occurrence of sulfide base metal mineralization, J. Geochem. Explor. 17 (1982) 49–62.

[50] W.R. Ryall, Anomalous trace elements in pyrite in the vicinity of mineralized zones of Woodlawn, N.S.W., Australia, J. Geochem. Explor. 8 (1977) 73–83.

[51] Z. Sawlowicz, Framboids: from their origin to application, Prace Mineralogiczne, Krakow (Mineral. Trans.) 88 (2000) 1–80.

[52] J. Schieber, The role of an organic slime matrix in the formation of pyritized burrow trails and pyrite concretions, Palaios 17 (2002) 104–109.

[53] M.A.A. Schoonen, H.L. Barnes, Reactions forming pyrite and marcasite from solutions: II. Via FeS precursors below 100 °C, Geochim. Cosmochim. Acta 55 (1991) 1505–1514.

[54] A. Seilacher, Concretion morphologies reflecting diagenetic and epigenetic pathways, Sediment. Geol. 143 (2001) 41–57.

[55] J. Selles-Martinez, Concretion morphology, classification and genesis, Earth-Sci. Rev. 41 (1996) 177–210.

[56] J.M. Skei, D.H. Loring, R.T.T. Rantala, Partitioning and enrichment of trace metals in a sediment core from Framvaren, South Norway, Mar. Chem. 23 (1988) 269–281.

[57] M. Soma, A. Tanaka, H. Seyama, K. Satake, Characterization of arsenic in lake sediments by X-ray photoelectron spectroscopy, Geochim. Cosmochim. Acta 58 (1994) 2743–2745.

[58] R.L. Stanton, Ore Petrology, McGraw-Hill, New York, 1972, 713 p.

[59] D.A.W. Stow, H.G. Reading, J.D. Collinson, Deep Seas, in: H.G. Reading (Ed.), Sedimentary Environments: Process, Facies and Stratigraphy, third ed., Blackwell, 1996, pp. 395–453.

[60] R.E. Sweeney, I.R. Kaplan, Pyrite framboid formation: laboratory synthesis and marine sediments, Econ. Geol. 68 (1973) 619–634.

[61] K.G. Taylor, J.H.S. Macquaker, Early diagenetic pyrite morphology in a mudstone-dominated succession: the Lower Jurassic Cleveland Ironstone Formation, eastern England, Sediment. Geol. 131 (2000) 77–86.

[62] S. Temur, Horzum (Kozan-Adana) ve Bolkardağı (Ulukışla-Niğde) yöreleri Zn–Pb yataklarına ait piritlerin iz element konsantrasyonlarının karşılaştırılması, in: S. Korkmaz, M. Akçay (Eds.), Jeoloji Müh. Bölümü 30, Yıl Sempozyomu Bildirileri, KTÜ-Trabzon, 1996, pp. 67–82.

[63] J.D. Vine, E.B. Tourtelot, Geochemistry of black shale deposits: A summary report, Econ. Geol. 65 (1970) 253–272.

[64] Q. Wang, J.W. Morse, Pyrite formation under conditions approximating those in anoxic sediments: I. Pathway and morphology, Mar. Chem. 52 (1996) 99–121.

[65] R.T. Wilkin, H.L. Barnes, Formation processes of framboidal pyrite, Geochim. Cosmochim. Acta 61 (1997) 323–339.

[66] E. Yilmaz, O. Duran, Güneydogu Anadolu Bölgesi Otokton ve Allokton Birimler Stratigrafi Adlama Sözlügü, TPAO Arastırma Merkezi Grubu Başkanligi Egitim Yayinlari, No. 31, 1997, 460 p.